Interconversions of the M, N, and O Intermediates in the Bacteriorhodopsin Photocycle†

György Váró,‡ Albert Duschl, and Janos K. Lanyi*
Department of Physiology and Biophysics, University of California, Irvine, California 92717
Received May 24, 1989; Revised Manuscript Received December 28, 1989

ABSTRACT: The reaction sequence in the second half of the bacteriorhodopsin (BR) photocycle (i.e., the steps which involve the M, N, and O intermediates) was investigated with a gated multichannel analyzer. The difference spectra, obtained between 0.4 and 25 ms after laser photoexcitation, were converted to absolute spectra of the mixtures of intermediates at each delay time. From these, the time courses of the concentrations of M, N, O, and BR in a single turnover were reconstructed. We found that in 1 M Na_2SO_4, between pH 4 and 7, the measurements were not complicated by multiple kinetic forms of M; thus, the progressive changes in the rise and decay kinetics of N and O, as well as the recovery of BR, with pH could be followed. The data are inconsistent with a linear sequence but suggest a model in which N is produced directly from M, and returns to BR via two pathways: (a) $O \rightleftarrows N \rightarrow BR$; (b) $N \rightleftarrows O \rightarrow BR$. The individual rate constants of the reactions vary characteristically with pH. Because of these variations, pathway a predominates at pH <6 and results in the increased transient accumulation of O by equilibration with N at acidic pH. Pathway b begins to contribute to pH >6 and results in the decreased accumulation of O but the increased accumulation of N at higher pH. Comparison of these results with the initial rate of proton transport between pH 4 and 7 indicates that proton translocation does not require that the BR photocycle pass through O.

Absorption of a photon by bacteriorhodopsin (BR),[1] the light-driven proton pump in the purple membrane of halobacteria (Stoeckenius et al., 1978; Stoeckenius & Bogomolni, 1982; Lanyi, 1984), results in the transient isomerization of the retinal chromophore from all-trans to 13-cis, the transient deprotonation of the retinal Schiff base, and the translocation of a proton across the membrane. The first half of the photoreaction cycle is characterized as a linear sequence of irreversible interconversions with decreasing rate constants at each successive step. Accordingly, the description of this part of the photocycle is fairly unambiguous: $BR \xrightarrow{h\nu} J \rightarrow K \rightarrow KL \rightarrow L$, where J, K, KL, and L are spectroscopically distinguishable species, and all reactions, but the first, are thermal interconversions on the femtosecond to nanosecond and microsecond time scales. The reactions in the second half of the reaction sequence are more ambiguous. They all occur on similar (millisecond) time scales, and a large body of data has suggested that this part of the photocycle contains reversible steps and/or branches. Because of the difficulties of interpreting such kinetics, the scheme which connects the spectroscopic species M, N, and O (or their possible multiple forms) had, until recently, remained elusive.

Within the last few years, difference spectra for another proposed photointermediate with an apparent absorption band in the UV (referred to as R; Dancshazy et al., 1986, 1987) and in the visible (referred to as P; Drachev et al., 1986) were reported. This species arose at alkaline pH, and on a time scale which would place it between M and BR. Because these difference spectra were similar to the difference spectrum of dark- vs light-adapted BR, one of us (J.K.L.) suggested that the intermediate represents a state in which the Schiff base is reprotonated but the retinal is still in the 13-cis configuration [as cited in Dancshazy et al. (1987)]. Kouyama et al. (1988) provided evidence that the form designated as R or P is, in fact, identical with what was previously described as N (Lozier et al., 1975), and proposed the scheme $M \rightarrow N \leftrightarrow O \leftrightarrow BR$, since the amounts of M and N produced in a single flash were so great that they could not arise in separate photocycles. Recently, evidence from Chernavskii et al. (1989) indicated that N and O must be in a rapid equilibrium. Also consistently with this scheme, Fodor et al. (1988) found that the decay of M matched the rise of N and the retinal in N was still 13-cis while in O it was already all-trans. However, Dancshazy et al. (1988) have proposed that N (R, P) at alkaline pH arises in a separate photocycle, in which it replaces M. In this scheme, the second photocycle is initiated from a different form of BR, which exists at higher pH.

The controversy over N is complicated by observations of multiple forms of M under various conditions. It has been known for some time that this spectroscopically distinct intermediate contains two kinetically resolved components: one which rises in ca. 50 μs and decays in 2–3 ms at neutral pH (M^f) and another which rises, at higher pH, in ca. 5 μs and decays, in a pH-dependent manner, between 5 ms and 1 s (M^s).[2] Kouyama et al. (1988) proposed a model in which M^s can be produced from N in a separate photocycle set off by the absorption of a second photon, since the lifetime of N is so greatly increased at high pH, and particularly at high salt concentrations, that under most illumination conditions a large fraction of BR exists as N. Again, Dancshazy et al. (1988) suggested a different model: M^f and M^s (and R, P,

† This work was supported by grants from the National Institutes of Health (GM 29498) and the U.S. Department of Energy (DE-FGOER 13525).
‡ Permanent address: Biological Research Center of the Hungarian Academy of Sciences, Szeged, Hungary.

[1] Abbreviations: BR, bacteriorhodopsin; HEPES, *N*-(2-hydroxyethyl)piperazine-*N*′-2-ethanesulfonic acid; MES, 2-(*N*-morpholino)-ethanesulfonic acid; Tris, tris(hydroxymethyl)aminomethane; TPP^+, triphenylphosphonium ion.

[2] Apparently because the rise of M^f is slower than the rise of M^s, the "fast M" in some publications is called "slow M" in others. In recent papers, the term "slow" and "fast" refer to the decay time of the M species in question.

0006-2960/90/0429-3798$02.50/0

or N) arise by single photon reactions from three different forms of BR, which are in pH-dependent thermal equilibrium with one another. As regards the two forms of M, this is the same interpretation as proposed by El-Sayed and co-workers (Hanamoto et al., 1984). While Kouyama et al. (1988) acknowledged that BR at high pH is in a thermal equilibrium with another form, which they suggested is N itself, they stated that only a small amount of N is produced in this way. Rather, they considered that the majority of N originates from the photocycle, and thus the majority of M^s is produced from BR after the absorption of two photons. Recent evidence (Ames et al., 1989) indicates, however, that M^s is produced also when a photoreaction of N does not take place and, furthermore, M^s might be only a kinetic entity rather than a distinct form of M.

In this paper, we report on the kinetics of the thermal interconversions of M, N, and O, under conditions where the M decay contains only a single exponential. With the reactions thus simplified, we could fit the data to a distinct model which describes the second half of the BR photocycle.

Materials and Methods

Purple membranes were isolated from *Halobacterium halobium* strain S9 according to Oesterhelt and Stoeckenius (1974). To prevent aggregation induced by salt, the samples were included in 4-mm-thick polyacrylamide gel slabs, using a method described by Mowery et al. (1979). The 570-nm absorbance of the purple membrane containing gels was 0.8. Their spectra agreed, within error, with spectra of purple membrane suspensions. Before the measurements, the gel slabs were equilibrated overnight in solutions of the pH of interest, which contained 1 M Na_2SO_4 plus 25 mM potassium acetate, MES, or Tris·HCl, depending on the pH.

All spectroscopic measurements were carried out at 22 °C after light adaptation of the bacteriorhodopsin. Transient spectra were measured as described elsewhere (Zimányi et al., 1989), with a gated optical multichannel analyzer (Princeton Instruments, Princeton, NJ). The excitation of the sample was with a nitrogen laser pumped dye laser (Model LN 1000/102, Photochemical Research Associates, London, Ontario, Canada). The data analysis was with an AST 286 desktop computer, using Lotus 123 software which allowed the numerical solution of differential equations and the simultaneous recalculation of all the spectra or concentrations considered.

Cell envelope vesicles containing BR, but negligible quantities of halorhodopsin, were prepared by in vitro reconstitution of bacterioopsin in *H. halobium* strain ET 1001/25 envelopes with *all-trans*-retinal (1.5 nmol/mg of protein). The envelopes were prepared in 4 M NaCl according to Lanyi and MacDonald (1979). For determining the dependence of proton transport on pH, the salt had to be exchanged for Na_2SO_4, and the internal pH changes during the illumination, as well as Na^+/H^+ antiport activity, needed to be eliminated. The first two were accomplished by loading the vesicles with osmotic shock by 2-h dialysis vs 1 M Na_2SO_4/80 mM $MnSO_4$ [for the latter, cf. Kouyama et al. (1987, 1988)], after which the excess Mn^{2+} was removed by dialysis vs 1 M Na_2SO_4. For the third, the vesicles were then heated to 55 °C for 5 min, followed by centrifugation for 30 min at 10000*g* and resuspension in 1 M Na_2SO_4, 0.2 mM TPP^+, and 2 mM buffer (either HEPES, MES, or citric acid). The assays for light-induced proton transport were done immediately after the resuspension, in a 3-mL volume at 2 mg/mL protein, as previously described (Duschl et al., 1988). The light intensity was adjusted with neutral density filters, and the absolute intensity was determined with a thermopile.

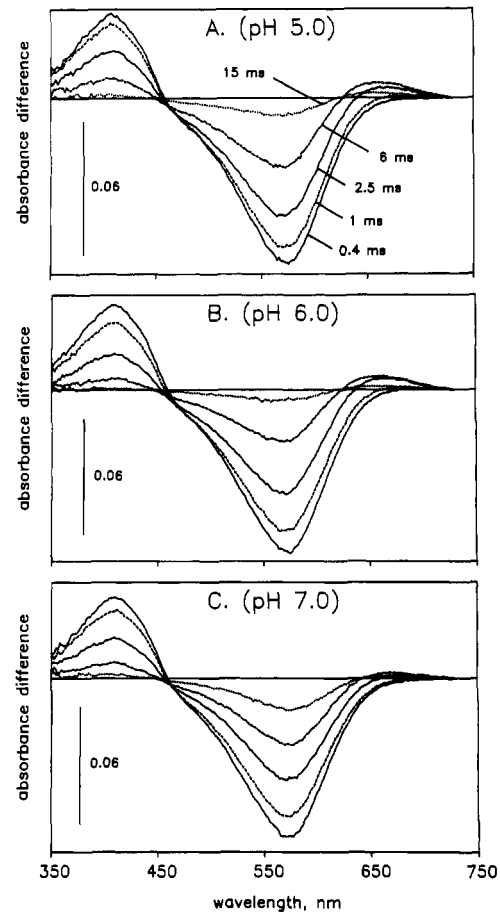

FIGURE 1: Flash-induced difference spectra at selected delay times between the photoexcitation and the measurement at pH 5.0 (A), pH 6.0 (B), and pH 7.0 (C). Conditions are described under Materials and Methods and Results. (—) 0.4 ms; (- - -) 1 ms; (—) 2.5 ms; (-·-) 6 ms; (···) 15 ms.

Results

Interconversions of M, N, O, and BR in the Bacteriorhodopsin Photocycle. A possible strategy for determining the reaction sequence in the second half of the photocycle is based on the known fact that the rates of the reactions vary with pH in such a way as to cause significant transient accumulation of O but not N at lower pH (Lozier et al., 1978; Li et al., 1984) and that of N but not O at higher pH (Kouyama et al., 1988). However, the results are complicated by complexities in the M kinetics: as the pH is increased, the rise and decay of M deviate more and more from a single exponential [e.g., see Lozier et al. (1978), Govindjee et al. (1980), and Hanamoto et al. (1984)]. It was fortunate, therefore, that we found conditions where the pH-dependent transition from a mainly O-containing to a mainly N-containing photocycle could be observed, while the slow kinetic form of M was virtually absent. This was achieved in the presence of 1 M Na_2SO_4 between pH 4 and 7, using purple membrane encased in a polyacrylamide gel to prevent its salt-induced aggregation (Váró & Lanyi, 1989). Figure 1 shows flash-induced difference spectra at pH 5, 6, and 7, at selected delay times in the 0.4–15-ms time range. Traces from two experiments at the same pH were superimposable. At each pH, the decay of M, whose absorption band is at 410 nm, was accompanied by the rise of other species, resulting in absorption increases at longer wavelengths. There were distinct progressive changes in these difference spectra with increasing

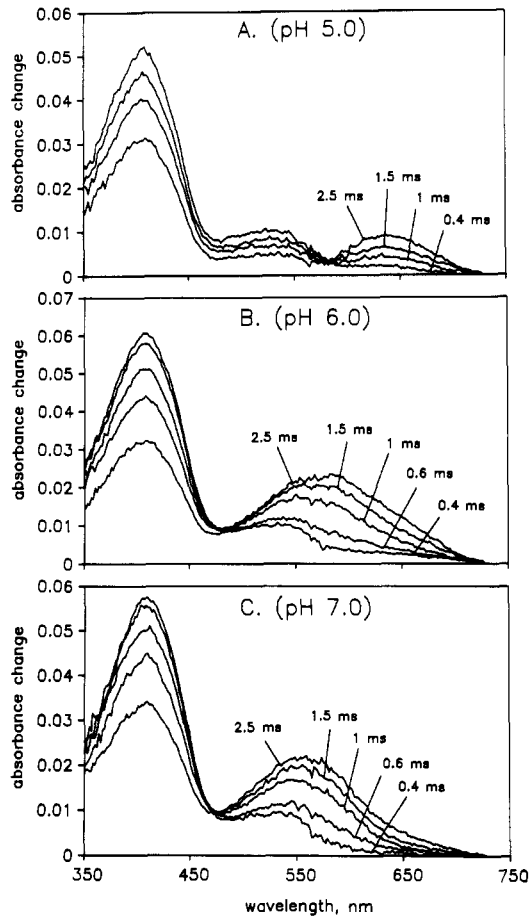

FIGURE 2: Absorption spectra of mixtures of intermediates at selected delay times between the photoexcitation and the measurement at pH 5.0 (A), pH 6.0 (B), and pH 7.0 (C). At each pH, the initial spectrum (0.4 ms) contains mainly the M spectrum (410-nm absorption band) *plus* a broad band between 500 and 550 nm of unknown origin, as discussed under Results. At subsequent times, up to 2.5 ms, the formation of O (at 640 nm, in panel A), the formation of N (at 560 nm, in panel C), or both (in panel B) are seen.

pH, most noticeably near 650 nm. The difference spectra at pH 4 were very similar to those at pH 5 (not shown). Between pH 4 and 7, there was no measurable shift (<1 nm) in the absorption band of the parent pigment. However, as found by others (Moore et al., 1978; Fischer & Oesterhelt, 1979; Mowery et al., 1979), at still lower pH the absorption maximum of BR exhibited a large red-shift (to 603 nm) under these conditions also, and the photoreactions of the so-called blue membrane produced were quite different (Váró & Lanyi, 1989).

By adding the spectrum of BR, with appropriate scaling factors, to these difference spectra, we obtained absolute spectra of the mixtures of intermediates present at each measured delay time after the photoexcitation. These spectra are shown in Figure 2 for pH 5, 6, and 7. The initial (0.4 ms) spectrum at each pH contains M, whose absorption maximum is near 410 nm; the possible origin of the second broad maximum between 500 and 550 nm is discussed below. The decrease of the initial absorption band(s) is accompanied by the rise (and subsequent decay, not shown in Figure 2 for clarity) of more than one species: at pH 5, an absorption band at 640 nm is produced (O); at pH 7, mostly an absorption band near 560 nm is produced (N); and at pH 6, both of these bands appear, but at earlier times, the mixtures contain more N and less O than at later times. Since the scaling factors for the BR spectra, used in producing these spectra (and others at intermediate pH values between 4 and 8; not shown), were

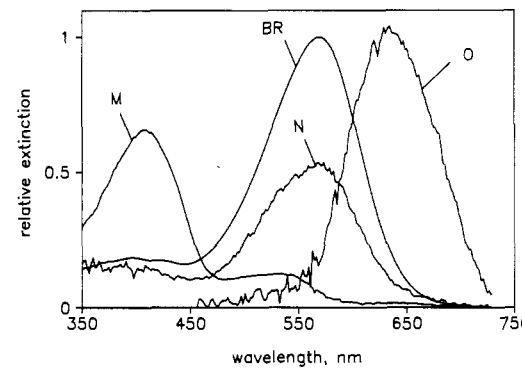

FIGURE 3: Calculated absorption spectra of the M, N, and O intermediates of the BR photocycle.

the only adjustable parameters, their correct choice was critical in this analysis. They were chosen by relying on isosbestic points. The spectra in Figure 2 are from delay times where little recovery of BR had yet taken place, and the only significant reactions were the interconversions of M, N, and O. Isosbestic points in the reconstructed spectra cannot be expected, naturally, once the recovery of BR begins. Thus, in spectra from later times, we obtained isosbestic points after multiplying the spectra by $1/(1-f)$, where 1 refers to the amount of BR bleached and f is the fraction of the bleached BR which had recovered. At the pH extremes, we assumed that only one intermediate besides M was seen (O or N), and thus the proper series of scaling factors was that which produced good isosbestic points (e.g., Figure 2A,C), either at 581 nm (between M and O) or at 474 nm (between M and N). At intermediate pH values, the criterion for chosing the scaling factors was that they should change smoothly with pH. Although not anticipated, the mixed spectra at intermediate pH (e.g., Figure 2B) contained nearly as good isosbestic points as the spectra containing only M and N, because the absorption of O near 474 nm is small (cf. below).

Since conditions (pH, delay time) existed where the absolute spectra of the intermediates seemed to contain no more than two species, i.e., M, N, or O, the spectra of these could be calculated. They are shown in Figure 3, together with the spectrum of BR for comparison, and agree with previous determinations of these spectra [e.g., see Lozier et al. (1975) and Lozier and Niederberger (1977)]: M absorbs at 408 nm (relative extinction 0.66), N absorbs at 560–570 nm (relative extinction 0.52), and O absorbs at 640 nm (relative extinction 1.03). The absorption maximum of BR in Figure 3 is 568 nm. As mentioned above, the calculated spectrum for M in Figure 3 contains a broad band between 500 and 550 nm [a similar spectrum for M was reported by Hess and Kuschmitz (1977), Zimányi et al. (1989), and Hofrichter et al. (1989)]. In treating the data as we do, we are assuming that if the absorption at 500–550 nm belongs to a minor, L-like intermediate and not to M itself, this intermediate is in rapid equilibrium with M on the time scale of the M decay [similarly to the way resonance Raman data were interpreted in Alshuth and Stockburger (1986)]. Accordingly, the ratio of this intermediate to M should not change after 0.4 ms; i.e., only the amplitude but not the shape of the composite spectrum containing M and the 500–550-nm species should vary with time. The justification for this assumption [in addition to the data in Alshuth and Stockburger (1986)] is that subtraction of the same composite M spectrum from each subsequent time-dependent spectrum produced invariant spectra for N and O.

The compositions of the mixtures of transient species at different times and different pH values were calculated in the

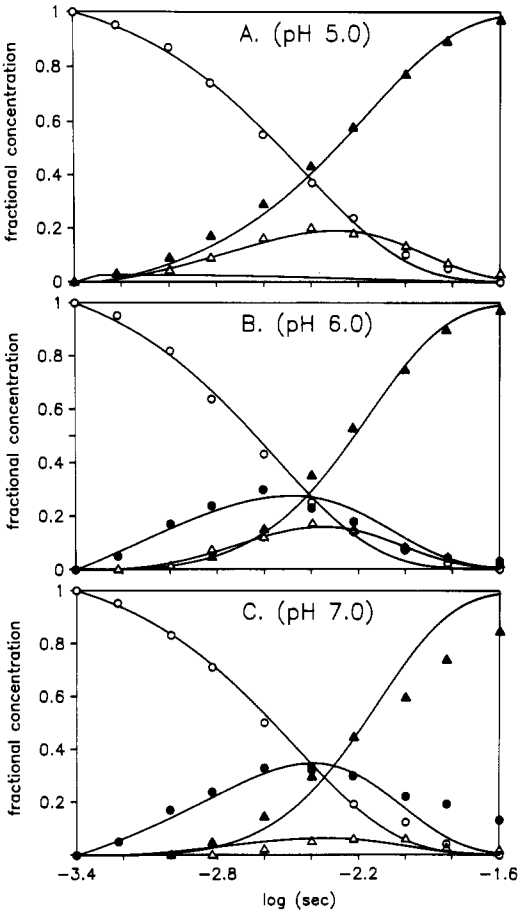

FIGURE 4: Time courses of M, N, O, and BR during a single pigment turnover, at pH 5.0 (A), 6.0 (B), and 7.0 (C). The amounts of the species are expressed as fractional concentrations, totaling 1. (○) M; (●) N; (△) O; (▲) BR. The lines represent predicted time courses, with rate constants appropriately chosen, as described in the text. The line in panel A without experimental points is the predicted time course of N at pH 5.0.

following way. Between 250 and 400 μs, the total amount of photoconverted BR was assumed to exist as M (except for the possibility of the minor, L-like species, as discussed above). This amount is given by the scaling factor appropriate at these times. The amounts of BR during its rise were given by the decrease in the scaling factors used for spectral reconstitutions at later times. The amounts of M and O could be estimated directly from the difference spectra, because their spectral overlap with all other species was minimal. Finally, the amounts of N were given by the difference between the total photoconverted pigment and the sum of the other species at the given time. As before (Zimányi et al., 1989), we express the contents of M, N, O, and BR as fractional concentrations between 0 and 1, where 1 refers to the amount of BR which had entered the photocycle. In Figure 4, these are plotted as functions of time after the flash. Thus, the data points in Figure 4 show, at pH 5, 6, and 7, time courses for the decay of M, followed by the rise and decay of N and O, and finally the rise of BR as the photocycle is concluded. As the pH was increased from 5 to 7, the relationships of these processes to one another were clearly and consistently altered: at pH 5, the O intermediate, but not N, was seen, and the rise of BR began immediately as M started to decay, but at pH 6, and even more at pH 7, N began to accumulate at the early part of the rise of O, while the rise of BR lagged further and further behind. From Figure 4, it is evident that the transient concentrations of N increased, and those of O decreased, with increasing pH. Although not shown, the rise of M was found

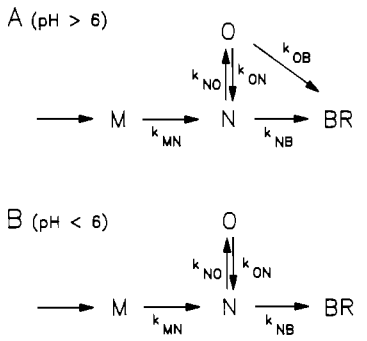

FIGURE 5: Models for the second half of the BR photocycle, consistent with the results in Figure 4, at pH >6 (A) and at pH <6 (B). The schemes are discussed in the text.

to be independent of pH in these experiments.

We attempted to fit the data in Figure 4, and similar data at other pH values between 4 and 7, to a kinetic model. The conventional method is to fit multiple exponential terms to the data, and evaluate the amplitudes and relaxation constants in terms of equations which describe the time-dependent concentrations of the intermediates in various models. We carried out such an analysis with data at pH 4 and 5, where the absence of observable amounts of N simplified matters. With a linear model, no unique solution was produced which satisfied each equation of an overdetermined system, and the partial solutions disagreed strongly with the data. On the other hand, we could obtain a solution with a model branched at N (cf. below), and it fit the data (not shown). However, this approach gave only approximations because exponential terms with amplitudes near zero could not be used in the calculations. Instead, we used a different method: we generated curves to fit the data, using the rate equations given in the Appendix, and systematically varied the rate constants until we were satisfied that the entire terrain of possible solutions was explored. In reducing the number of alternative schemes, we took into account the following general considerations: (a) O was placed after N, since under most conditions the beginning of the rise of O occurred when N was already present; (b) reversible reactions between O and BR, and between N and BR, were excluded by the fact that these would have led to thermal equilibria containing O or N even before any illumination, and shifts in the spectrum of purple membrane were not observed between pH 4 and 7. Other than these points, we considered a complete scheme where all interconversions were allowed. Many of the reactions were then excluded because the simulations predicted kinetics incompatible with the data, as explained under Discussion. This analysis left the scheme in Figure 5A, where the M → N reaction is followed by an N ↔ O equilibrium and the N → BR reaction, but O decays also via the O → BR pathway. This scheme is consistent with the results of the exponential fitting, described above. As stated in the Appendix, the rate constants for the steps were designated as k with the subscripts MN, NO, NB, ON, and OB, for the M → N, N → O, N → BR, O → N, and O → BR reactions, respectively. The rate constants were adjusted, using the exhaustive search strategy mentioned above, until the best agreement of the calculated curves (lines, from numerical integrations) with the data (points), shown in Figure 4, was obtained. The satisfactory fit under all conditions, except at times beyond 10 ms at pH 7, defined the five rate constants. The deviation from a good fit was even more serious at pH higher than 7 (not shown), and we attribute it to the considerable slowing down of the N decay at higher pH (Kouyama et al., 1988; Kouyama-Nasuda & Kouyama, 1989; Váró & Lanyi, 1990). At these pH values, the model in Figure

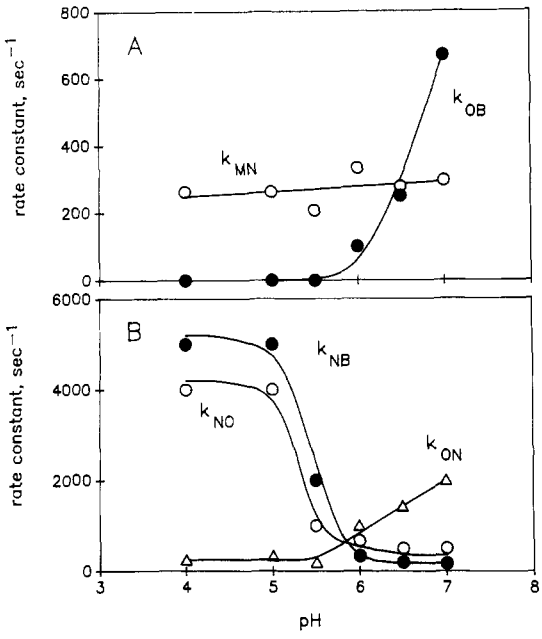

FIGURE 6: pH dependencies of the calculated rate constants shown in Figure 5. Data from experiments such as shown in Figure 4. (A) (○) k_{MN}; (●) k_{OB}; (B) (○) k_{NO}; (●) k_{NB}; (△) k_{ON}.

5 no longer explains the data.

Figure 6 shows the rate constants as functions of pH. These exhibit different pH dependencies, depending on the reactants, but not the products, in the reactions: k_{MN} is relatively pH invariant, k_{NO} and k_{NB} show large decreases with an apparent pK of 5.4, and k_{ON} and k_{OB} show large increases above pH 6. The result of the pH-dependent changes in the rate constants is that below pH 6 M decays to BR entirely via the M → N → BR pathway, even as O accumulates via its equilibration with N (Figure 5B). This is because fitting the data requires that k_{OB} be zero at low pH. Thus, it is only above pH 6 that the linear M → N ↔ O → BR pathway (Figure 5A) begins to contribute significantly. The fraction of BR generated directly via the N → BR reaction is shown, as a function of pH, in Figure 7.

pH Dependence of Proton Transport. Although in some reports [e.g., see Lozier and Niederberger (1977), Lozier et al. (1978), and Li et al. (1984)] the rate of light-driven proton translocation in BR-containing vesicles dropped significantly as the pH was raised, Kouyama and Nasuda-Kouyama (1989) recently suggested that this is an effect of the rise of intravesicle pH on the photocycle. The latter authors found that the inherent rate of proton transport was, in fact, fairly pH independent up to pH 7. We determined the initial rate of proton extrusion in illuminated cell envelope vesicles containing BR, but largely lacking halorhodopsin, in 1 M Na_2SO_4. Following the suggestions of Kouyama and Nasuda-Kouyama (1989), we took care to eliminate spurious influences on the inherent proton transport rate: the vesicles were internally buffered with Mn^{2+}, sodium/proton exchange activity and proton permeability were reduced by heat treatment of the vesicles, and a low light intensity (4 mW/cm^2) was used. The results, in Figure 7, show that when these precautions were observed, proton transport was fairly independent of pH under the conditions of the above-described spectroscopic measurements.

Discussion

Measurements of the kinetics of absorption changes at single wavelengths have produced a large number of models, but

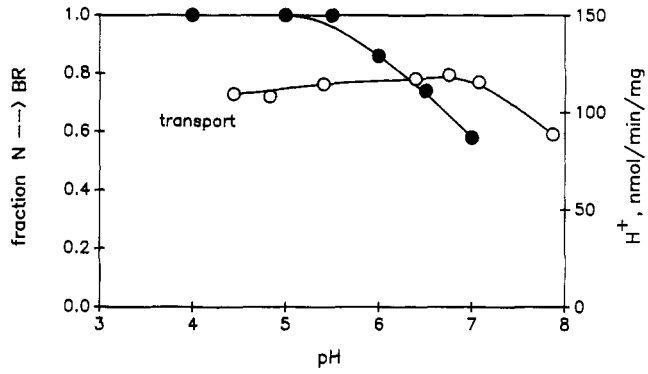

FIGURE 7: pH dependencies of the branching of the BR photocycle and of light-driven proton transport. (●) The calculated fraction of M which decays to BR via the direct route M → N → BR (rather than the alternative, M → N ↔ O → BR, as shown in Figure 5); (○) initial rate of proton extrusion in illuminated *H. halobium* envelope vesicles (light intensity 4 mW/cm^2), determined as described under Materials and Methods.

limited understanding, of the exact sequence of the complex interconversions in the second half of the BR photocycle. We attempted to solve this problem by obtaining high-resolution transient difference spectra with an optical multichannel analyzer (Figure 1). Model-independent, absolute methods for interpreting such data have been tried (Mauer et al., 1987a,b; Hofrichter et al., 1989), but the complexity of the kinetic problem and the overlap of the relaxations have not yet allowed firm conclusions. Instead, our approach was to decompose the spectra into their component spectra corresponding to the known photointermediates of BR (Figure 3). The criteria used for this decomposition, as given under Results, are highly important, and the validity of the results depends on their correct use. The results obtained gave time courses for the concentrations of M, N, O, and BR in a single turnover of the pigment, and they were found to vary with pH (Figure 4). Following this, we considered a general kinetic scheme in which most of the possible reactions were allowed, generated solutions from these from the rate equations, and eliminated those steps incompatible with the data.

The result of the above analysis is a kinetic model in which N is produced directly from M and returns to BR via two pathways: (a) O ↔ N → BR; (b) N ↔ O → BR (Figure 5). Pathway b corresponds to the linear scheme for M, N, and O, widely assumed for the BR photocycle, while pathway a excludes O from the reaction sequence leading to BR. The pH dependency of the rate constants in these sequences (Figure 6) revealed that at acid pH pathway a predominated but at increasing pH above 6 pathway b began to contribute as well (Figure 7). Presumably, at still higher pHs, pathway b takes over entirely, but here the model could not explain a second, slow component in the decay of N (Figure 4C). A linear pathway at all pH values was rejected because in kinetic simulations it predicted either a delayed rise for BR relative to the rise of O (if $k_{OB} \ll k_{NO}$) or a rapid rise for BR but no accumulation of O (if $k_{OB} \gg k_{NO}$). The data indicated that neither of these applied: O accumulated, while the beginning of the rise of BR coincided with the rise of O (Figure 4A,B). Similarly, a linear pathway predicted that, independently of the rate constants, the decay of O should extend beyond the decay of N. According to the data (e.g., Figure 4B), the decay of O and N coincided in time.

In disregarding some possible interconversions, we were guided by the principle that they must be excluded in at least one pH domain, and they should not be necessary to invoke at other pH values. Thus, direct conversion of M into BR was

excluded at pH ≥6, because the rise of BR lagged significantly behind the beginning of the decay of M (Figure 4B,C). At pH <6, this reaction is allowed by the observed kinetics (Figure 4A), but introducing it into the rate equations did not make for a better fit to the time courses of N and O, while those changes in the rate constants (Figure 6), which provide such a fit, fully accounted also for the data points for M in this pH region. Therefore, even though not strictly ruled out at pH <6, we feel that a direct M → BR reaction is unlikely. The back-reaction, N → M, which is likely to occur at higher pH (Várô & Lanyi, 1990), was excluded under the conditions used, because it would have caused biphasic M decay, which was not observed in this study. Finally, the direct conversion of M into O was excluded, because a significant decay of M was seen to occur before the beginning of the rise of O (Figure 4B). Additionally to the last point, as mentioned under Results, whenever N was seen to accumulate, its rise always preceded the rise of O (Figure 4B,C).

In the proposed kinetic model (Figure 5), the pH dependency of the rate constants exhibits an unexpected self-consistency. The results (Figure 6) reveal that the rates of both reactions of N (i.e., N → O and N → BR) show a large decrease with a midpoint at pH 5.3–5.4. Similarly, the rates of both reactions of O (i.e., O → N and O → BR) show large increases, although well above pH 5.5. The pH dependencies of k_{NO} and k_{ON} are thus not mirror images of one another, as expected if the N ↔ O reaction included proton transfer to and from the medium. The M → N reaction is relatively pH independent. While the protein residues, and/or lipid groups, which play roles in these pH dependencies are not yet known, it seems clear that specific ionization states must exist in purple membrane, which direct the course of reactions in the second part of the photocycle.

Recently, experiments by Chernavskii et al. (1989) indicated that when excess O was caused to suddenly accumulate by applying a thermal (IR laser) pulse, it reequilibrated with N much faster than the rate of its conversion to BR. This result puts a restriction on the rate constants in Figure 5. We simulated such a perturbation in our model by increasing k_{NO} and decreasing k_{NB} for 40 μs near the maximum accumulation of O. The result (not shown) indicated that at pH 6 and 7 (although not at lower pH), the original O kinetics resumed rapidly after such a perturbation, much in the way found by Chernavskii et al. (1989). Thus, the model in Figure 5 is compatible with the results of these authors.

Once the two pathways for the recovery of BR were described, our intention was to decide which, if not both, is associated with proton translocation. Earlier results on the pH dependencies of the accumulation of O and transport (Lozier et al., 1978; Li et al., 1984) suggested a correlation of this intermediate and proton translocation. However, we found that while the fraction of M which decayed via the direct M → N → BR pathway declined with increasing pH above 5, and the fraction which decayed through O increased, transport remained fairly constant (Figure 7). Thus, both pathways of N decay in Figure 5 must be associated with proton translocation; i.e., the transport of protons does not require that O be in the reaction sequence between M and BR.

Appendix

In the kinetic analysis, we first considered all reactions allowed by considerations a and b listed under Results. Thus, the general scheme contained the following interconversions: M ↔ N, M ↔ O, N ↔ O, N → BR, O → BR, and M → BR. Accordingly, the equations which describe the kinetics were as follows:

$$d[M]/dt = k_{OM}[O] + k_{NM}[N] - (k_{MO} + k_{MN} + k_{MB})[M] \quad (1)$$

$$d[N]/dt = k_{MN}[M] + k_{ON}[O] - (k_{NM} + k_{NO} + k_{NB})[N] \quad (2)$$

$$d[O]/dt = k_{MO}[M] + k_{NO}[N] - (k_{OM} + k_{ON} + k_{OB})[O] \quad (3)$$

$$[M] + [N] + [O] + [BR] = 1 \quad (4)$$

The initial conditions were [M] = 1 and [N] = [O] = [BR] = 0. By setting one or more of the rate constants to zero, the numerical solutions of these equations generated predictions for the time courses of [M], [N], [O], and [BR] in each of the alternative models we considered. The grounds for rejecting the individual reactions, N → M, M ↔ O, and M → BR, under the conditions of these measurements are listed under Discussion.

Registry No. H, 12408-02-5.

References

Alshuth, T., & Stockburger, M. (1986) *Photochem. Photobiol. 43*, 55–66.

Ames, J. B., Fodor, S. P. A., Gebhard, R., Raap, J., van den Berg, M. M., Lugtenburg, J., & Mathies, R. A. (1989) *Biochemistry 28*, 3681–3687.

Chernavskii, D. S., Chizhov, I. V., Lozier, R. H., Murina, T. M., Prokhorov, A. M., & Zubov, B. V. (1989) *Photochem. Photobiol. 49*, 649–653.

Dancshazy, Zs., Govindjee, R., Nelson, B., & Ebrey, T. G. (1986) *FEBS Lett. 209*, 44–48.

Dancshazy, Zs., Govindjee, R., & Ebrey, T. G. (1987) in *Biophysical Studies of Retinal Proteins* (Ebrey, T. G., Frauenfelder, H., Honig, B., & Nakanishi, K., Eds.) pp 167–173, University of Illinois Press, Urbana–Champaign, IL.

Dancshazy, Zs., Govindjee, R., & Ebrey, T. G. (1988) *Proc. Natl. Acad. Sci. U.S.A. 85*, 6358–6361.

Drachev, L. A., Kaulen, A. D., Skulachev, V. P., & Zorina, V. V. (1986) *FEBS Lett. 209*, 316–320.

Duschl, A., McCloskey, M. A., & Lanyi, J. K. (1988) *J. Biol. Chem. 263*, 17016–17022.

Fischer, U., & Oesterhelt, D. (1979) *Biophys. J. 28*, 211–230.

Fodor, S. P., Ames, J. B., Gebhard, R., van der Berg, E. M., Stoeckenius, W., Lugtenburg, J., & Mathies, R. A. (1988) *Biochemistry 27*, 7097–7101.

Govindjee, R., Ebrey, T. G., & Crofts, A. R. (1980) *Biophys. J. 30*, 231–242.

Hanamoto, J. H., Dupuis, P., & El-Sayed, M. A. (1984) *Proc. Natl. Acad. Sci. U.S.A. 81*, 7083–7087.

Hess, B., & Kuschmitz, D. (1977) *FEBS Lett. 74*, 20–24.

Hofrichter, J., Henry, E. R., & Lozier, R. H. (1989) *Biophys. J. 56*, 693–706.

Kouyama, T., & Nasuda-Kouyama, A. (1989) *Biochemistry 28*, 5963–5970.

Kouyama, T., Nasuda-Kouyama, A., & Ikegami, A. (1987) *Biophys. J. 51*, 839–841.

Kouyama, T., Nasuda-Kouyama, A., Ikegami, A., Mathew, M. K., & Stoeckenius, W. (1988) *Biochemistry 27*, 5855–5863.

Lanyi, J. K. (1984) in *Comparative biochemistry: bioenergetics*, (Ernster, L., Ed.) pp 315–350, Elsevier, Amsterdam.

Lanyi, J. K., & MacDonald, R. E. (1979) *Methods Enzymol. 55*, 777–780.

Li, Q., Govindjee, R., & Ebrey, T. G. (1984) *Proc. Natl. Acad. Sci. U.S.A. 81*, 7079–7082.

Lozier, R. H., & Niederberger, W. (1977) *Fed. Proc., Fed. Am. Soc. Exp. Biol. 36*, 1805-1809.
Lozier, R. H., Bogomolni, R. A., & Stoeckenius, W. (1975) *Biophys. J. 15*, 955-963.
Lozier, R. H., Niederberger, W., Ottolenghi, M., Sivorinovsky, G., & Stoeckenius, W. (1978) in *Energetics and Structure of Halophilic Microorganisms* (Caplan, S. R., & Ginzburg, M., Eds.) pp 123-139, Elsevier/North-Holland, Amsterdam.
Mauer, R., Vogel, J., & Schneider, S. (1987a) *Photochem. Photobiol. 46*, 247-253.
Mauer, R., Vogel, J., & Schneider, S. (1987b) *Photochem. Photobiol. 46*, 255-262.
Moore, T. A., Edgerton, M. E., Parr, G., Greenwood, C., & Perham, R. N. (1978) *Biochem. J. 171*, 469-476.
Mowery, P. C., Lozier, R. H., Chae, Q., Tseng, Y. W., Taylor, M., & Stoeckenius, W. (1979) *Biochemistry 18*, 4100-4107.
Oesterhelt, D., & Stoeckenius, W. (1974) *Methods Enzymol. 31*, 667-678.
Stoeckenius, W., & Bogomolni, R. A. (1982) *Annu. Rev. Biochem. 51*, 587-616.
Stoeckenius, W., Lozier, R. H., & Bogomolni, R. A. (1978) *Biochim. Biophys. Acta 505*, 215-278.
Váró, Gy., & Lanyi, J. K. (1989) *Biophys. J. 56*, 1143-1151.
Váró, Gy., & Lanyi, J. K. (1990) *Biochemistry 29*, 2241-2250.
Zimányi, L., Keszthelyi, L., & Lanyi, J. K. (1989) *Biochemistry 28*, 5165-5172.

Guanine Nucleotide Binding Characteristics of Transducin: Essential Role of Rhodopsin for Rapid Exchange of Guanine Nucleotides†

Ahmad B. Fawzi* and John K. Northup‡
Department of Pharmacology, Yale University School of Medicine, 333 Cedar Street, New Haven, Connecticut 06510
Received August 21, 1989; Revised Manuscript Received December 5, 1989

ABSTRACT: Transducin (G_t) is a member of a family of receptor-coupled signal-transducing guanine nucleotide (GN) binding proteins (G-proteins). Light-activated rhodopsin is known to catalyze GN exchange on G_t, resulting in the formation of the active state of the $G_{t\alpha}$–GTP complex. However, purified preparations of G_t have been shown to exchange GN in the absence of activated receptors [Wessling-Resnick, M., & Johnson, G. L. (1987) *Biochemistry 26*, 4316-4323]. To evaluate the role of rhodopsin in the activation of G_t, we studied GN-binding characteristics of different preparations of G_t. G_t preparations obtained from the supernate of GTP-treated bovine rod outer segment (ROS) disks, followed by removal of free GTP on a Sephadex G-25 column, bound GTPγS at 30 °C in the absence of added exogenous rhodopsin with an activity of 1 mol of GTPγS bound/mol of G_t (G_t-I preparations). Binding of GTPγS to G_t-I preparations closely correlated with the activation of ROS disk cGMP phosphodiesterase. GN-binding activity of G_t-I preparations was dependent on reaction temperature, and no binding was observed at 4 °C. In the presence of 10 μM bleached rhodopsin, G_t-I preparations bound GTPγS at 4 °C. However, hexylagarose chromatography of G_t-I preparations led to a preparation of G_t that showed <0.1 mol/mol binding activity following 60-min incubation at 30 °C in the absence of rhodopsin (G_t-II preparations). In the presence of as low as 0.03 μM bleached rhodopsin, G_t-II preparations rapidly bound GTPγS at 30 °C. Equimolar mixtures of G_t-I and G_t-II preparations showed a 1.0 mol/mol binding activity in the absence of added rhodopsin. While treatment of G_t-I preparations with hydroxylamine, which is known to convert rhodopsin to opsin, greatly diminished the rate of GTPγS binding to the preparation, addition of 0.03 μM bleached rhodopsin following removal of hydroxylamine restored the binding activity. These results indicate that (1) rhodopsin is essential for rapid GN exchange on G_t and (2) rapid GN exchange in the absence of exogenous rhodopsin observed in some G_t preparations is stimulated by undetected rhodopsin contamination.

Signals generated by hormones and neurotransmitters at the level of cell surface receptors are now well-known to be transmitted through a family of highly homologous GTP-binding proteins (G-proteins)[1] [for review, see Gilman (1984, 1987)]. Hormonal activation and inhibition of the enzyme adenylate cyclase and light activation of retinal rod outer segment (ROS) cGMP phosphodiesterase (PDE) are among the best characterized receptor–effector systems coupled through G-proteins. The G-proteins G_s and G_i couple stimulatory and inhibitory receptors, respectively, to the enzyme adenylate cyclase. In the homologous system of visual signal transduction, light-activated rhodopsin is coupled to retinal ROS G-protein transducin (G_t). Receptor-coupled G-proteins are heterotrimeric proteins composed of α, β, and γ-subunits.

†Supported by a grant from NIH (GM40154) and in part by BRSG Grant PR 05358 awarded by the Biomedical Research Support Grant Program, Division of Research Resources, National Institutes of Health.
‡Established Investigator of the American Heart Association.

[1] Abbreviations: G-protein, a member of the family of signal-transducing GTP-binding regulatory proteins; G_t, vertebrate retinal G-protein (transducin); G_s and G_i, stimulatory and inhibitory GTP-binding proteins of the adenylate cyclase system, respectively; G_o, 39-kDa GTP-binding protein of high abundance in the brain; ROS, rod outer segment; PDE, phosphodiesterase; cGMP, guanosine 3′,5′-cyclic monophosphate; GN, guanine nucleotides; GTPγS, guanosine 5′-*O*-(3-thiotriphosphate); Gpp(NH)p, guanosine 5′-(β,γ-imidotriphosphate); EDTA, ethylenediaminetetraacetic acid; MOPS, 4-morpholinepropanesulfonic acid; Tris, tris(hydroxymethyl)aminomethane; PMSF, phenylmethanesulfonyl fluoride; DTT, dithiothreitol; SDS, sodium dodecyl sulfate; BSA, bovine serum albumin; TCA, trichloroacetic acid; PPO, 2,5-diphenyloxazole.

0006-2960/90/0429-3804$02.50/0